

REPORT

PALEOANTHROPOLOGY

The earliest modern humans outside Africa

Israel Hershkovitz,^{1,2,*} Gerhard W. Weber,^{3,†} Rolf Quam,^{4,5,6,†} Mathieu Duval,^{7,8} Rainer Grün,^{7,9} Leslie Kinsley,⁹ Avner Ayalon,¹⁰ Miryam Bar-Matthews,¹⁰ Helene Valladas,¹¹ Norbert Mercier,¹² Juan Luis Arsuaga,^{5,13} María Martín-Torres,^{14,15,16} José María Bermúdez de Castro,^{8,14} Cinzia Fornai,^{3,17} Laura Martín-Francés,^{8,18} Rachel Sarig,^{2,19} Hila May,^{1,2} Viktoria A. Krenn,^{3,17} Viviane Slon,¹ Laura Rodríguez,^{5,20,21} Rebeca García,^{5,20} Carlos Lorenzo,^{22,23} Jose Miguel Carretero,^{5,20} Amos Frumkin,²⁴ Ruth Shahack-Gross,²⁵ Daniella E. Bar-Yosef Mayer,^{26,27} Yaming Cui,²⁸ Xinzhi Wu,²⁸ Natan Peled,²⁹ Iris Groman-Yaroslavski,³⁰ Lior Weissbrod,³⁰ Reuven Yeshurun,³⁰ Alexander Tsatskin,³⁰ Yossi Zaidner,^{30,31} Mina Weinstein-Evron³⁰

To date, the earliest modern human fossils found outside of Africa are dated to around 90,000 to 120,000 years ago at the Levantine sites of Skhul and Qafzeh. A maxilla and associated dentition recently discovered at Misiya Cave, Israel, was dated to 177,000 to 194,000 years ago, suggesting that members of the *Homo sapiens* clade left Africa earlier than previously thought. This finding changes our view on modern human dispersal and is consistent with recent genetic studies, which have posited the possibility of an earlier dispersal of *Homo sapiens* around 220,000 years ago. The Misiya maxilla is associated with full-fledged Levallois technology in the Levant, suggesting that the emergence of this technology is linked to the appearance of *Homo sapiens* in the region, as has been documented in Africa.

The timing and routes of modern human migration out of Africa are key issues for understanding the evolution of our own species. The fossil evidence suggests that the earliest members of the *Homo sapiens* clade (Jebel Irhoud, Omo, and Herto) appeared in Africa during the late Middle Pleistocene (1–4). Outside Africa, modern humans appeared much later, during the Late Pleistocene in the Levant (Qafzeh, Skhul) (5–7), and possibly in East Asia (Daioxian) (8). Misiya Cave, Israel, is part of a complex of prehistoric caves along the western slopes of Mount Carmel (Fig. 1 and fig. S1). Here we report on an adult hominin left hemimaxilla (Misiya-1) (Fig. 2A) found in Square N9 of the upper part of the Early Middle Palaeolithic (EMP) archaeological layer of the site (Stratigraphic Unit 6, Upper Terrace, Fig. 1 and fig. S1), associated with an Early Levantine Mousterian (Tabun D type) stone-tools assemblages (9, 10). Misiya-1 preserves much of the alveolar and zygomatic processes, part of the palate and nasal floor, and the complete left dentition from the first incisor (represented by a broken root only) to the third molar (Fig. 2A).

Three independent numerical dating methods—U-series (U-Th), combined uranium series and electron spin resonance (US-ESR) series, and thermoluminescence (TL)—carried out in three different dating laboratories yielded consistent results (Fig. 2B, figs. S2 and S3, and tables S1 and S3). A series of nine TL dates on burned flints

from Square L10 and N12 in the vicinity of the human fossil (Fig. 1, A and B) provided a mean age of 179 ± 48 thousand years (ky) (2σ) (range = 212 to 140 ky) (11). U-Th analyses of the dentine of the I² from the maxilla and of the crust adhering directly to the maxilla yielded a minimum age of 70.2 ± 1.6 ky (2σ ; table S1) and 185 ± 8.0 ky (2σ ; Fig. 2B and table S2), respectively (9). The combined US-ESR dating of the enamel of the same tooth yielded a maximum age of 174 ± 20 ky (2σ) (Fig. 2B, fig. S3, and tables S1 and S3) (9). All these dates, except for the U-series dating of the dentine, which exclude the possibility of recent intrusion, fall within the time range for the Early Levantine Mousterian lithic industry (Tabun D-type) observed at Tabun, Hayonim, and Misiya caves (i.e., ~250 to ~140 ky) (11–13) and are older than the upper range defined for the EMP sequence in Misiya Cave (>165 ky) (11). Collectively, the evidence suggests an early marine isotope stage 6 (MIS 6) age for the Misiya-1 fossil. The age range for Misiya-1, based on dates directly connected with the fossil (U-Th on crust providing the minimum boundary and the maximum boundary of US-ESR on the enamel of I²), is between 177 and 194 ky [for details and calculation methods, see (9) and fig. S2].

The insertion of the zygomatic root in Misiya-1 is relatively anteriorly placed, at the level of M¹, similar to recent *H. sapiens* as well as the fossils from Herto and Jebel Irhoud (1, 3). The zygomatico-alveolar crest is strongly curved and inserts at a

low position relative to the dentition. Three-dimensional (3D) geometric morphometric (GM) analysis (9) of the maxillary morphology (Fig. 3A) shows that Misiya-1 is similar to modern humans and is most dissimilar to Neandertals and some Middle Pleistocene hominins. Based on the logarithm of the centroid size of the 3D data (9), Misiya-1 is smaller than all fossil *Homo* specimens in our sample and falls in the range of variation observed for recent modern humans. In addition, the anterior placement of the incisive foramen, the sloped or level nasal floor configuration, and the shape of the dental arcade in Misiya-1 (Fig. 2A)

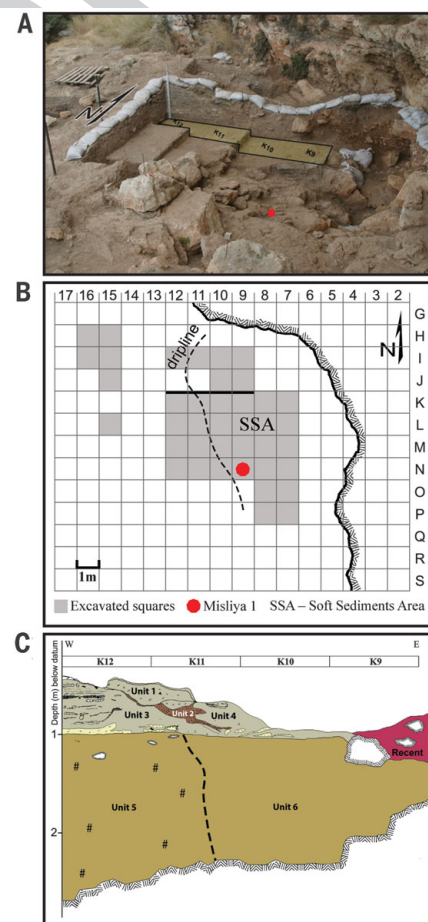


Fig. 1. The Misiya Cave excavation area at the Upper Terrace of the cave and the stratigraphy. (A) The excavation area and the location of the Misiya-1 maxilla (red dot). Squares K9 to K12 are indicated. (B) Map of the Misiya Cave Upper Terrace excavations (1 m² grid) with denoted excavated squares and showing the location of the human maxilla (Misiya-1). (C) Stratigraphic section of the Upper Terrace, squares K9 to K12. Apart from Unit 2, a Terra Rosa soil intrusion, all units contain EMP finds or assemblages. The present-day diaphane roughly separates between highly cemented (Units 1,3,5) and more loosely cemented (Units 4 and 6) sediments. Misiya-1 was retrieved from the upper part of Unit 6.

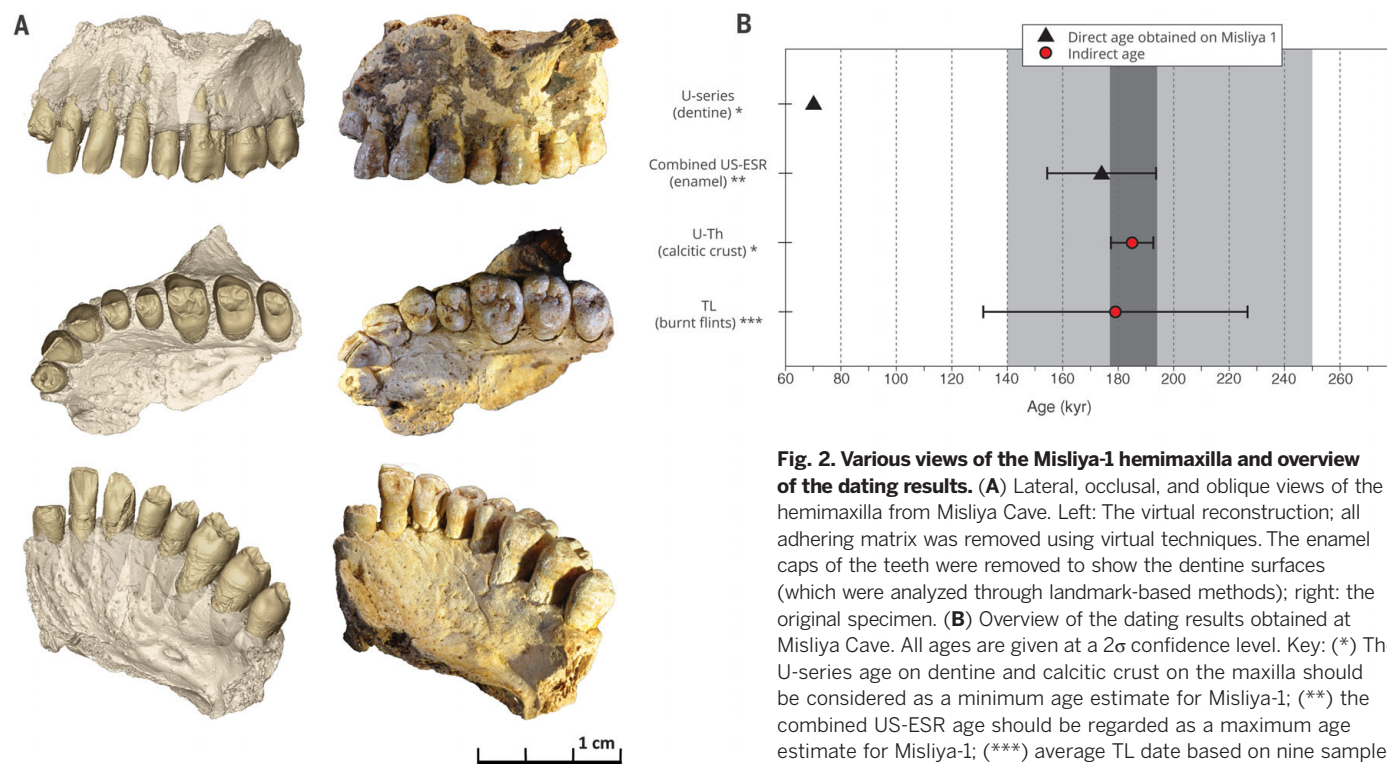


Fig. 2. Various views of the Misliya-1 hemimaxilla and overview of the dating results. (A) Lateral, occlusal, and oblique views of the hemimaxilla from Misliya Cave. Left: The virtual reconstruction; all adhering matrix was removed using virtual techniques. The enamel caps of the teeth were removed to show the dentine surfaces (which were analyzed through landmark-based methods); right: the original specimen. **(B)** Overview of the dating results obtained at Misliya Cave. All ages are given at a 2σ confidence level. Key: (*) The U-series age on dentine and calcitic crust on the maxilla should be considered as a minimum age estimate for Misliya-1; (**) the combined US-ESR age should be regarded as a maximum age estimate for Misliya-1; (***) average TL date based on nine samples of burned flint obtained from nearby squares (N12, L10; see Fig. 1).

Dark gray: Age range for Misliya-1, based on dates directly obtained from the fossil itself (U-Th provides the minimum age and combined US-ESR the maximum age), is between 177 ky ($=185 - 8$ ky) to 194 ky ($=174 + 20$ ky). Light gray: Age range for the EMP period in the Levant (250 to 140 ky) based on the combination of TL dates obtained for Tabun Cave (13), Hayonim Cave (12), and Misliya Cave (11).

are characteristic of modern humans, although individual features can occasionally be found in earlier taxa.

The I^2 (Fig. 2A and fig. S4) shows several features that are characteristic of *H. sapiens* (14), including a flat labial surface [labial convexity grades 0 or 1, scoring based on Arizona State University Dental Anthropology System (ASUDAS)], a straight incisal edge, very slight shoveling (ASUDAS grade 1), and lack of a lingual tubercle. The presence of a lingual groove can also be found in Pleistocene *H. sapiens* samples such as Qafzeh and Huanglong. The canine lacks the mass-additive traits typical of Asian *Homo erectus* (15), Middle

Pleistocene European specimens, and Neandertals, and resembles Qafzeh and Skhul. Unlike Neandertals canines, the shovel shape is not pronounced, and there is no lingual tubercle or mesial canine ridge (Fig. 2A).

The upper premolars display relatively simple occlusal surfaces and lack accessory marginal tubercles and buccal cingulum (Fig. 2A). The Misliya-1 premolars display the typical high and narrow crown of *H. sapiens*. In the occlusal view, the P^3 shows a slight lingual narrowing, which is less pronounced in the P^4 . This contrasts with the characteristic Neandertal pattern featuring a low and broad crown and subequal buccal and

lingual aspects of the crown in both upper premolars. The proportion of occlusal area (defined by the occlusal rim) is large relative to the crown base area in the upper premolars of Misliya-1, unlike in Neandertals, where the occlusal area appears compressed relative to the crown base area. This compression in Neandertal upper premolars is homologous to the relative reduction of the occlusal polygon found in Neandertal M^1 s (16, 17), and this latter feature is absent in Misliya-1.

The Misliya-1 maxillary teeth are within the upper size range of modern humans (table S5). Size proportions between the anterior and posterior

¹Department of Anatomy and Anthropology, Sackler Faculty of Medicine, Tel Aviv University, Post Office Box 39040, Tel Aviv 6997801, Israel. ²The Dan David Center for Human Evolution and Biohistory Research and The Shmunis Family Anthropology Institute, The Steinhardt Museum of Natural History, Tel Aviv University, Post Office Box 39040, Tel Aviv 6997801, Israel. ³Department of Anthropology, University of Vienna, Althanstrasse 14, A-1090 Vienna, Austria; Core Facility for Micro-Computed Tomography, University of Vienna, Althanstrasse 14, A-1090 Vienna, Austria. ⁴Department of Anthropology, Binghamton University (SUNY), Binghamton, NY 13902-6000, USA. ⁵Centro UCM-ISCIII de Investigación sobre la Evolución y Comportamiento Humanos, Avda. Monforte de Lemos, 5, 28029, Madrid, Spain. ⁶Division of Anthropology, American Museum of Natural History, Central Park West at 79th Street, New York, NY 10024-5192, USA. ⁷Australian Research Centre for Human Evolution (ARCHE), Environmental Futures Research Institute, Griffith University, Nathan QLD 4111, Australia. ⁸Centro Nacional de Investigación sobre la Evolución Humana (CENIEH), Paseo de la Sierra de Atapuerca 3, 09002, Burgos, Spain. ⁹Research School of Earth Sciences, The Australian National University, Canberra ACT 2601, Australia. ¹⁰Geological Survey of Israel, 30 Malkhe Israel Street, Jerusalem 9550161, Israel. ¹¹Laboratoire des Sciences du Climat et de l'Environnement, LSCE/IPSL, CEA-CNRS-UVSQ, Université Paris-Saclay, avenue de la terrasse, 91198 Gif sur Yvette Cedex, France. ¹²Institut de Recherche sur les Archéomatériaux, UMR 5060 CNRS - Université de Bordeaux Montaigne, Centre de Recherche en Physique Appliquée à l'Archéologie (CRP2A), Maison de l'archéologie, 33607 PESSAC Cedex, France. ¹³Departamento de Paleontología, Facultad de Ciencias Geológicas, Universidad Complutense de Madrid, Ciudad Universitaria s/n, 28040, Madrid, Spain. ¹⁴Department of Anthropology, University College London, 14 Tavistock Street, London, WC1H 0BW, UK. ¹⁵Departamento de Ciencias Históricas y Geografía, Universidad de Burgos, Facultad de Humanidades y Educación, 09001, Burgos, Spain. ¹⁶National Research Center on Human Evolution (CENIEH), Paseo Sierra de Atapuerca 3, 09002 Burgos, Spain. ¹⁷Institute of Evolutionary Medicine, University of Zurich, Winterthurerstrasse 190, CH-8057 Zurich, Switzerland. ¹⁸UMR5189 PACEA Université de Bordeaux MCC, France. ¹⁹Department of Oral biology and Orthodontics, the Maurice and Gabriela Goldschleger School of Dental Medicine, Sackler Faculty of Medicine, Tel Aviv University, 6997801 Israel. ²⁰Departamento de Historia, Geografía y Comunicación, Universidad de Burgos, Facultad de Humanidades y Educación, 09001, Burgos, Spain. ²¹Facultade de Humanidades, Universidad Isabel I, Spain. ²²Àrea de Prehistoria, Universitat Rovira i Virgili, Avinguda Catalunya 35, 43002 Tarragona, Spain. ²³Institut Català de Paleoeologia Humana i Evolució Social (IPHES), Marcel·lí Domingo s/n, 43007 Tarragona, Spain. ²⁴Institute of Earth Science, The Hebrew University of Jerusalem, Jerusalem 9190401, Israel. ²⁵Department of Maritime Civilizations, Recanati Institute of Maritime Studies, University of Haifa, Haifa, Mount Carmel 3498838, Israel. ²⁶Sonia and Marco Nadler Institute of Archaeology Tel Aviv University, Tel Aviv 69978, Israel. ²⁷Peabody Museum of Archaeology and Ethnology, Harvard University, 11 Divinity Avenue, Cambridge, MA 02138, USA. ²⁸Department of Paleontology, Institute of Paleontology and Paleoanthropology, Chinese Academy of Science, Str. Xizhimenwai no. 144, 100044 Beijing, China. ²⁹Department of Radiology, Carmel Medical Center, Haifa, 3436212 Israel. ³⁰Zinman Institute of Archaeology, University of Haifa, Haifa, Mount Carmel 3498838, Israel. ³¹Institute of Archaeology, The Hebrew University of Jerusalem, Jerusalem 9190501, Israel.

*Corresponding author. Email: anat02@tauex.tau.ac.il †These authors contributed equally to this work.

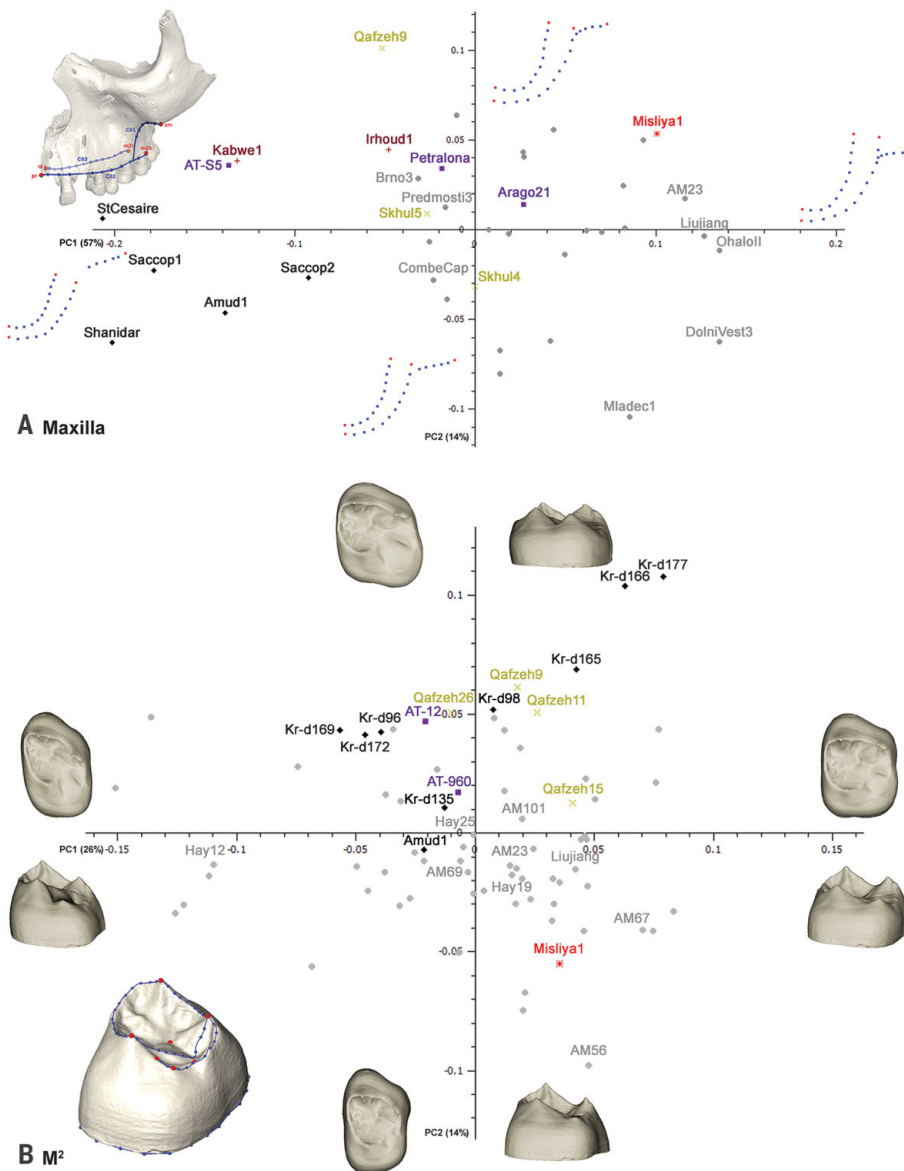


Fig. 3. First two principal components (PCs) in shape space and associated warped surfaces at the extremities of the axes. Noteworthy shape changes in the warpings are as follows: **(A)** Maxillary bone. PC1, anterior-posterior position and angle of the zygomatic root. PC2, curvature of the zygomatico-alveolar crest. **(B)** Upper M²; PC2, relative expansion and height of the hypocone; buccolingual relative size of the EDJ occlusal area to the crown base. On the left side of each of the plots, the landmark configurations used for the respective anatomical unit are represented (landmarks in red, curve semilandmarks and pseudolandmarks on CEJ in blue). Prosthion (pr), orale (ol), zygomaxillare (zm), midpoint of the M² alveolar socket buccally (m2b) and lingually (m2l); upper region of the zygomaticoalveolar crest (C01); buccal alveolar margin (C02), lingual alveolar margin (C03). Red star, Misliya-1; gray circles, recent modern humans (without labels), Upper Paleolithic and Epipaleolithic modern *Homo* (with labels); black diamonds, Neandertals; yellow X, early modern humans; violet square, European Early and Middle Pleistocene *Homo*; burgundy plus sign, African Early and Middle Pleistocene *Homo*; for the specimen labels, refer to table S7.

teeth differentiate Misliya-1 from Neandertals (fig. S5). The buccolingual (BL) size ratio of the I² to M¹ in Misliya-1 (62.6) is just outside the upper limit of the range of modern humans (mean = 55.6, SD = 3.4, $n = 31$, range = 48.2 to 62.5), is similar to the mean of Qafzeh and Skhul (mean = 63.4, SD = 4.9, $n = 9$, range = 56.1 to 71.4), and well

below the lower limit of the range of Neandertals (mean = 70.3, SD = 3.1, $n = 13$, range = 66.7 to 76.0). Therefore, Misliya-1 does not exhibit the relative expansion of the anterior dentition characteristic of Neandertals (18). Tooth root size and morphology are also within the range of modern humans (fig. S4).

Two-dimensional GM analysis (9) of the M¹ crown outline (Fig. 4) reveals that Misliya-1 is separate from Neandertals and other European Middle Pleistocene hominins, placing it with modern humans and near to Jebel Irhoud. It differs from Neandertals as well as from other European Middle Pleistocene fossils by not displaying the skewed rhomboidal crown outline and large and protruding hypocone. The relative sizes of the M¹ protocone and hypocone align Misliya-1 with modern humans and differentiate it from Neandertals (table S4).

The 3D GM analysis (9) of the premolars, including the enamel-dentine junction (EDJ) occlusal area and cementum-enamel junction (CEJ) (fig. S6), shows that the Misliya-1 premolars are located in quadrants exclusively occupied by *H. sapiens*, with the exception of one Atapuerca Sima de los Huesos (SH) P³ (that is located in the same quadrant but far from Misliya-1) and the P⁴ of Amud 1. A similar analysis of the Misliya-1 M² (Fig. 3B) places it in an area exclusively occupied by contemporary *H. sapiens* (and the Liujiang specimen), which are characterized by a reduction of the hypocone and a buccolingually widened (rectangular) crown base. This contrasts with what is observed in Neandertals and most other European Middle Pleistocene fossils where the hypocone is relatively more developed. The Qafzeh specimens are quite variable but uniformly display a larger hypocone than does Misliya-1. The strong reduction of the hypocone observed in M¹ (table S4), M², and M³ of Misliya-1 is most frequently observed in *H. sapiens*, although it can occasionally be found in other *Homo* groups (17, 18).

Overall, the Misliya-1 teeth are distinct from those of the Middle Pleistocene specimens from Europe, Africa, and Asia such as Atapuerca (SH), Steinheim, Rabat, Qesem Cave, Chaoxian, and Xujiayao. Although some dental features seen in Misliya-1 can occasionally also be found in some of these samples, the entire suite of metric and morphological traits seen in the Misliya-1 maxillary bone and teeth is more consistent with *H. sapiens* than with Neandertals or other Middle Pleistocene hominin groups. Indeed, the combination of features in the incisor and canine appears to occur only in *H. sapiens* (19).

Middle Pleistocene fossils from southwest Asia (e.g., Qesem Cave, Zuttiyeh) are rare and display a mixture of features considered characteristic of Neandertals or modern humans, thus complicating their taxonomic assignment (20–22). Although incomplete, the Misliya-1 maxilla does not exhibit any derived skeletal or dental Neandertal features. A specific comparison with the earlier teeth from Qesem Cave (20, 21) reveals a number of differences. Specifically, the Qesem I² shows a pronounced lingual tubercle, greater degree of labial curvature, and more pronounced shoveling, whereas the Qesem C¹ shows more pronounced shoveling, a lingual tubercle, and a canine mesial ridge. All of these features are more commonly found in Neandertal anterior teeth and represent points of departure from the morphology seen in Misliya-1 teeth. In contrast, Misliya-1 resembles the later Levantine *H. sapiens* fossils from the

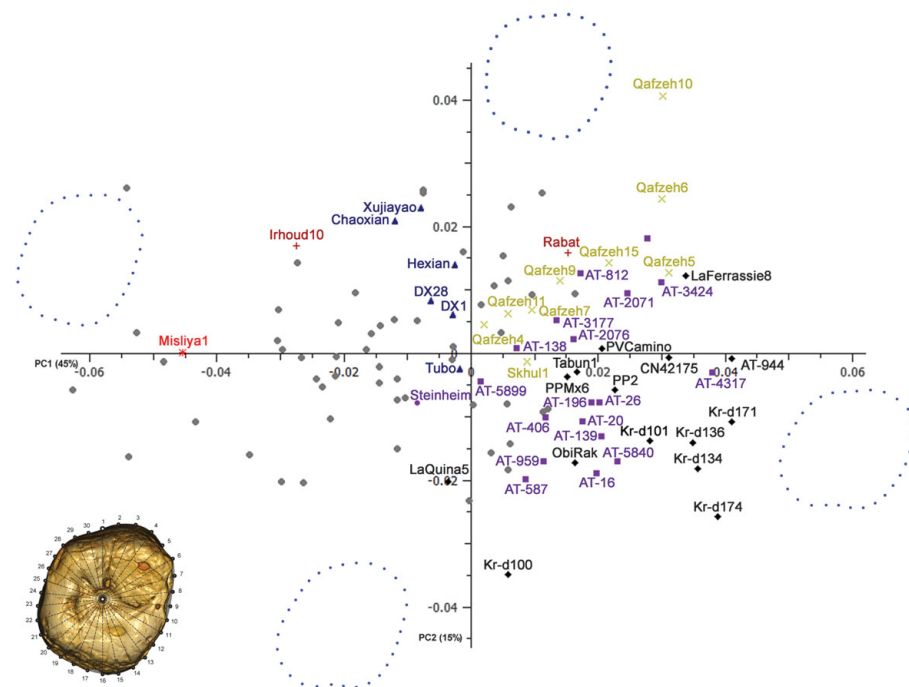


Fig. 4. First two principal components (PCs) of the crown shape of Misliya-1 M¹. Misliya-1 is distinct from Neandertals and other Middle Pleistocene hominins and clearly grouped with modern humans. Red star, Misliya-1; gray circles, recent modern humans (without labels), Upper Paleolithic and Epipaleolithic modern *Homo* (with labels); black diamonds, Neandertals; yellow X, early modern humans; violet square, European Early and Middle Pleistocene *Homo*; burgundy plus sign, African Early and Middle Pleistocene *Homo*; blue triangle, Middle Pleistocene Asian specimens; for the specimen labels, refer to table S7.

sites of Skhul and Qafzeh regarding many dental features, but it also differs from them regarding the degree of hypocone reduction seen in Misliya-1.

The geographical origin, timing, and identification of the last common ancestor of Neandertals and modern humans remain controversial (23, 24). Nevertheless, the evolutionary emergence of Neandertals in Europe from their Middle Pleistocene precursors [e.g., Atapuerca (SH), Steinheim, Ehringsdorf] is better established, despite the possibility that more than one lineage coexisted in the European Middle Pleistocene (25). The geographical origin of *H. sapiens* is generally considered to be Africa, and the Jebel Irhoud fossils, recently dated to ~300 ky ago (2), are thought to represent an “early phase of *H. sapiens* evolution” [(1), p. 291]. Younger fossils from the sites of Omo (~195 ky ago) and Herto (~160 ky ago) have been attributed to *H. sapiens* (3, 4). Nevertheless, the African fossil records reveal temporal overlaps between more “archaic” and more “modern” forms of early *H. sapiens* (24). These African specimens are thought to be members of the *H. sapiens* clade, even though some of them fall outside the range of variation of Holocene humans regarding certain features (3, 24). Similarly, many of the teeth, which are thought to represent early *H. sapiens* from North Africa, retain primitive features (26).

Misliya-1 considerably pushes back the timing of the earliest migration of members of the *H. sapiens* clade out of Africa, well predating

Qafzeh and Skhul in the Levant, and Daoxian and Liujiang in China [(8) and (27); but see (28)].

Archaeologically, the EMP layers of Misliya cave document the emergence of novel technological concepts in the Levant, including full-fledged Levallois technology and laminar technology (29). Similar technological concepts have been documented at contemporary and earlier Middle Stone Age sites in Africa, i.e., the Maghreb (Jebel Irhoud), eastern Africa (Gademotta and Kulakuletti formations, Ethiopia, and the Kaphurin Formation, Kenya), and southern Africa (Kathu Pan) (2, 30–34). Thus, similar to the recent findings from Jebel Irhoud (1, 2), the evidence from Misliya Cave suggests that the emergence of full-fledged Levallois technology in the Levant may have also been associated with the occurrence of *H. sapiens*.

The region of southwest Asia represents a major biogeographic corridor for hominin migrations during our evolutionary history. Given the geographical proximity of the Levant to Africa, it is possible that the dispersals documented at Misliya Cave (177 to 194 ky ago), Qafzeh and Skhul Caves (90 to 120 ky ago), and Manot Cave (50 to 60 ky ago) reflect expansions of the geographical range of *H. sapiens*, fluctuating in response to demographic or environmental factors (35).

To date, Misliya-1 appears to represent the earliest fossil evidence of the migration of members of the *H. sapiens* clade out of Africa. It therefore opens the door to the possibility that *H. sapiens*

dispersal from Africa could have occurred earlier than previously thought (probably before 200 ky ago), as has been recently suggested based on genetic evidence (36).

REFERENCES AND NOTES

1. J.-J. Hublin et al., *Nature* **546**, 289–292 (2017).
2. D. Richter et al., *Nature* **546**, 293–296 (2017).
3. T. D. White et al., *Nature* **423**, 742–747 (2003).
4. I. McDougall, F. H. Brown, J. G. Fleagle, *Nature* **433**, 733–736 (2005).
5. N. Mercier et al., *J. Archaeol. Sci.* **20**, 169–174 (1993).
6. C. B. Stringer, R. Grün, H. P. Schwarcz, P. Goldberg, *Nature* **338**, 756–758 (1989).
7. H. P. Schwarcz et al., *J. Hum. Evol.* **17**, 733–737 (1988).
8. W. Liu et al., *Nature* **526**, 696–699 (2015).
9. Materials and methods are available as supplementary materials at Science online.
10. Y. Zaidner, M. Weinstein-Evron, *Before Farm.* **2012**, 1–23 (2012).
11. H. Valladas et al., *J. Hum. Evol.* **65**, 585–593 (2013).
12. N. Mercier et al., *J. Archaeol. Sci.* **34**, 1064–1077 (2007).
13. N. Mercier, H. Valladas, *J. Hum. Evol.* **45**, 401–409 (2003).
14. M. Martínón-Torres et al., *Proc. Natl. Acad. Sci. U.S.A.* **104**, 13279–13282 (2007).
15. F. Weidenreich, *Nature* **1**, 269–272 (1937).
16. S. E. Bailey, *J. Hum. Evol.* **47**, 183–198 (2004).
17. M. Martínón-Torres, J. M. Bermúdez de Castro, A. Gómez-Robles, L. Prado-Simón, J. L. Arsuaga, *J. Hum. Evol.* **62**, 7–58 (2012).
18. J. M. Bermúdez de Castro, M. E. Nicolas, *Am. J. Phys. Anthropol.* **96**, 335–356 (1995).
19. S. E. Bailey, J. Hublin, in *Anthropological Perspectives on Tooth Morphology: Genetics, Evolution, Variation*, G. Scott, J. Irish, Eds. (Cambridge Univ. Press, Cambridge, 2013), pp. 222–249.
20. G. Weber et al., *Quat. Int.* **398**, 159–174 (2016).
21. I. Hershkovitz et al., *Am. J. Phys. Anthropol.* **144**, 575–592 (2011).
22. S. E. Freidline, P. Gunz, I. Janković, K. Harvati, J.-J. Hublin, *J. Hum. Evol.* **62**, 225–241 (2012).
23. A. Gómez-Robles, J. M. Bermúdez de Castro, J.-L. Arsuaga, E. Carbonell, P. D. Polly, *Proc. Natl. Acad. Sci. U.S.A.* **110**, 18196–18201 (2013).
24. C. Stringer, *Philos. Trans. R. Soc. Lond. B Biol. Sci.* **371**, 1698 (2016).
25. J. L. Arsuaga et al., *Science* **344**, 1358–1363 (2014).
26. S. E. Bailey, T. D. Weaver, J. Hublin, in *Human Paleontology and Prehistory*, A. Marom, E. Hovers, Eds. (Springer International, Cham, Switzerland, 2017), pp. 215–232.
27. G. Shen et al., *J. Hum. Evol.* **43**, 817–829 (2002).
28. W. Liu, X. Wu, L. Wang, *Acta Anthropol. Sin.* **25**, 177–194 (2006).
29. M. Weinstein-Evron, Y. Zaidner, A. Tsatskin, R. Yeshurun, I. Hershkovitz, in *Quaternary of the Levant: Environments, Climate Change, and Humans*, Y. Enzel, O. Bar-Yosef, Eds. (Cambridge Univ. Press, Cambridge, 2017), pp. 225–230.
30. K. Douze, A. Delagnes, *J. Hum. Evol.* **91**, 93–121 (2016).
31. C. R. Johnson, S. McBrearty, *J. Hum. Evol.* **58**, 193–200 (2010).
32. N. Porat et al., *J. Archaeol. Sci.* **37**, 269–283 (2010).
33. Y. Sahle, L. E. Morgan, D. R. Braun, B. Atafu, W. K. Hutchings, *Quat. Int.* **331**, 6–19 (2014).
34. C. A. Tryon, S. McBrearty, P.-J. Texier, *Afr. Archaeol. Rev.* **22**, 199–229 (2005).
35. I. Hershkovitz et al., *Nature* **520**, 216–219 (2015).
36. C. Posth et al., *Nat. Commun.* **8**, 16046 (2017).

ACKNOWLEDGMENTS

Field work in Misliya Cave was supported by the Dan David Foundation, the Irene Levi-Sala CARE Archaeological Foundation, the Leakey Foundation, the Thyssen Foundation, and the Faculty of Humanities of the University of Haifa. Laboratory work and dating were supported by the Israel Science Foundation (grant no. 1104/12). The anthropological study was supported by the Dan David Foundation, Ministerio de Economía y Competitividad of Spain (MINECO: CGL2015-65387-C3-3-P), Fundación Atapuerca, and The Leakey Foundation. The ESR dating study received funding from the Marie Curie International Outgoing Fellowship (IOF) 626474 and the Australian Research Council Future Fellowship FT150100215. N.M. is grateful to LaScArBx ANR-10-LABX-52 for support. Work on the virtual specimens was supported by the Life Science Faculty University of Vienna; Österreichische Nationalbank, Anniversary

Fund, project no. 16121; the Swiss National Science Foundation grant nos. 31003A 156299/1 and 31003A 176319; A.E.R.S. Dental Medicine Organizations GmbH, Vienna, Austria, project no. FA547014; and the Siegfried Ludwig–Rudolf Slavicek Foundation, Vienna, Austria, project no. FA547016. Special thanks are due to the late Dan David and his son, Ariel David, for their inspiration and financial support throughout the years. Thanks also go to O. Bar-Yosef (Harvard University) and A. M. Tillier (University of Bordeaux), who read and commented on a previous version of this paper. All data generated in this study are in the supplementary materials. Permission to study the fossil (Misliya-1) can be obtained from the corresponding author. Micro-CT images are available from G.W.W. under a material transfer agreement with I.H. of Tel Aviv University (Misliya-1). Full acknowledgments are in the

supplementary materials. I.H. and M.W.-E. direct the Misliya Cave research project; I.H., G.W.W., R.Q., J.L.A., M.M.-T., J.M.B.dC., L.M.-F., P.S., R.S., H.M., V.S., L.R., R.G., C.L., J.M.C., Y.C., X.W., and N.P. carried out various aspects of the anthropological study of the Misliya human remains; G.W.W., C.F., V.A.K., and R.S. carried out the virtual image manipulation and geometric morphometric investigations; Y.Z. and M.W.-E. conducted the archaeological studies at the cave; A.A. and M.B.-M. conducted the U/Th analysis; H.V. and N.M. conducted the TL dating of the archaeological layers; M.D., R.G., and L.K. conducted the U-series and ESR dating of the fossil remains; A.F., R.S.-G., and A.T. conducted the geoarchaeological and geomorphological studies of the cave; L.W. and R.Y. conducted the study of the faunal remains; D.B.-Y.M. studied the mollusc shells; and I.G.-Y. carried out the use-wear

analysis. All authors participated in compiling the manuscript. The authors declare no competing financial interests.

SUPPLEMENTARY MATERIALS

www.sciencemag.org/content/vol/issue/page/suppl/DC1
Materials and Methods
Supplementary Text
Acknowledgments
Figs. S1 to S6
Tables S1 to S7
References (37–114)

31 August 2017; accepted 21 December 2017
10.1126/science.aap8369